

# A Two-Tier Control Architecture for Nonlinear Process Systems with Continuous/Asynchronous Feedback

Jinfeng Liu, David Muñoz de la Peña, Benjamin J. Ohran, Panagiotis D. Christofides and James F. Davis

**Abstract**—In this work, we introduce a two-tier control architecture for nonlinear process systems with both continuous and asynchronous sensing and/or actuation. This class of systems arises naturally in the context of process control systems based on hybrid communication networks (i.e. point-to-point wired links integrated with networked wired/wireless communication) and utilizing multiple heterogeneous measurements (e.g., temperature and concentration). Assuming that there exists a lower-tier control system which relies on point-to-point communication and continuous measurements to stabilize the closed-loop system, we propose to use Lyapunov-based model predictive control to design an upper-tier networked control system to profit from both the continuous and the asynchronous measurements as well as from additional networked control actuators. The proposed two-tier control system architecture preserves the stability properties of the lower-tier controller while improving the closed-loop performance. The theoretical results are demonstrated using a chemical process example.

## I. INTRODUCTION

Increasingly faced with the requirements of safety, environmental sustainability, and profitability, chemical process operation is relying extensively on highly automated control systems. Traditionally, control systems utilize point-to-point wired communication links using a small number of sensors and actuators. The operation of chemical processes, therefore, could benefit from the deployment of control systems using hybrid communication networks that take advantage of an efficient integration of the existing, point-to-point communication networks (wire connections from each actuator/sensor to the control system using dedicated local area networks) and additional networked (wired or wireless) actuator/sensor devices. Such an augmentation in sensor information and networked based availability of wired and wireless data is now well underway in the process industries [1], [2], [3] and clearly has the potential to be transformative in the sense of dramatically improving the ability of the single-process and plantwide model-based control systems to optimize process and plant performance (in terms of achieving control objectives that go well beyond the ones

that can be achieved with control systems using wired, point-to-point connections) and prevent or deal with adverse and emergency situations more quickly and effectively (fault-tolerance). Hybrid communication networks allow for easy modification of the control strategy by rerouting signals, having redundant systems that can be activated automatically when component failure occurs, and in general, they allow having a high-level supervisory control over the entire process [1], [2], [3]. However, augmenting existing control networks with real-time wired/wireless sensor and actuator networks challenges many of the assumptions in traditional process control methods dealing with dynamical systems linked through ideal channels with flawless, continuous communication. In the context of hybrid communication networks which utilize networked sensors and actuators, key issues that are important for process control include robustness, reliability and interference. These issues need to be carefully handled because integrated wired and wireless communication networks introduce more components in order to substantially improve closed-loop performance and fault-tolerance, and this increases the probability of missing data at any given point in time.

Within control theory, the study of control over networks has attracted considerable attention in the literature [4], [5] and early research focused on analyzing and scheduling real-time network traffic [6], [7]. Research has also studied the stability of network-based control systems. A common approach is to insert network behavior between the nodes of a conventional control loop. In [8] it was proposed to first design the controller using established techniques considering the network transparent, and then to analyze the effect of the network on closed-loop system stability and performance. This approach was further developed in [9] using a small gain analysis approach. However, the available results on network-based control have primarily utilized wired networks. In the last few years, however, several research papers have studied control using the IEEE 802.11 and Bluetooth wireless networks, see [10] and the references therein. In the design and analysis of networked control systems, the most frequently studied problem considers control over a network having constant and time-varying delays. This network behavior is typical of communications over the Internet but does not necessarily represent the behavior of dedicated wireless networks in which the sensor, controller, and actuator nodes communicate directly with one another but might experience data losses. An appropriate framework to model lost data, is the use of asynchronous systems [11], [12]. In this framework, data losses occur in an stochastic

Financial support from NSF, CBET-0529295 and MCYT, DPI2007-66718-C04-01, is gratefully acknowledged.

Jinfeng Liu, Benjamin J. Ohran, Panagiotis D. Christofides and James F. Davis are with the Department of Chemical and Biomolecular Engineering, University of California, Los Angeles, CA 90095-1592, USA. Panagiotis D. Christofides is also with the Department of Electrical Engineering, University of California, Los Angeles, CA 90095-1592, USA, jinfeng@ucla.edu, ohran@ucla.edu, pdc@seas.ucla.edu, jdavis@conet.ucla.edu.

David Muñoz de la Peña is with the Departamento de Ingeniería de Sistemas y Automática Universidad de Sevilla, Sevilla 41092, Spain, dmunoz@us.es.

manner, and the process is considered to operate in an open-loop fashion when data is lost. The most destabilizing cause of packet loss is due to bursts of poor network performance in which case large groups of packets are lost nearly consecutively. A more detailed description of bursty network performance using a two-state Markov chain was considered in [13]. Modeling networks, using Markov chains results in describing the overall closed-loop system as a stochastic hybrid system [14]. Stability results have been presented for particular cases of stochastic hybrid systems in [15], [16]. In the MPC framework, several different control schemes for systems subject to asynchronous measurements have been proposed [17], [18]. However, these results do not directly address the problem of augmentation of dedicated, wired control systems with networked actuator/sensor devices to improve closed-loop performance.

In this work, we introduce a two-tier control architecture for nonlinear process systems with both continuous and asynchronous sensing and/or actuation. This class of systems arises naturally in the context of process control systems based on hybrid communication networks (i.e., point-to-point wired links integrated with networked wired/wireless communication) and utilizing multiple heterogeneous measurements (e.g., temperature and concentration). Assuming that there exists a lower-tier control system which relies on point-to-point communication and continuous measurements to stabilize the closed-loop system, we propose to use Lyapunov-based model predictive control to design an upper-tier networked control system to profit from both the continuous and the asynchronous measurements as well as from additional networked control actuators. The proposed two-tier control system architecture preserves the stability properties of the lower-tier controller while improving the closed-loop performance. The theoretical results are demonstrated using a chemical process example.

## II. PRELIMINARIES

### A. Problem formulation

In this work, we consider nonlinear systems described by the following state-space model

$$\begin{aligned}\dot{x}(t) &= f(x(t), u_s(t), u_a(t), w(t)) \\ y_s(t) &= h_s(x(t)) \\ y_a(t) &= h_a(x(t))\end{aligned}\quad (1)$$

where  $x(t) \in R^{n_x}$  denotes the vector of state variables,  $y_s(t) \in R^{n_{y_s}}$  denotes continuous and synchronous measurements,  $y_a(t) \in R^{n_{y_a}}$  are asynchronous and sampled measurements,  $u_s(t) \in R^{n_{u_s}}$  and  $u_a(t) \in R^{n_{u_a}}$  are two different sets of possible control inputs and  $w(t) \in R^{n_w}$  denotes the vector of disturbance variables. The disturbance vector is bounded, i.e.,  $w(t) \in W$  where

$$W := \{w \in R^{n_w} \text{ s.t. } |w| \leq \theta, \theta > 0\}^1.$$

We assume that  $f$  is a locally Lipschitz vector function,  $h_s$  and  $h_a$  are sufficiently smooth functions,  $f(0, 0, 0, 0) = 0$ ,

<sup>1</sup> $|\cdot|$  denotes Euclidean norm of a vector.

$h_s(0) = 0$  and  $h_a(0) = 0$ . This means that the origin is an equilibrium point for the nominal system (system (1) with  $w(t) \equiv 0$  for all  $t$ ) with  $u_s = 0$  and  $u_a = 0$ .

### B. Modeling of measurements/network

As we have mentioned before, system (1) is controlled using both continuous synchronous and sampled asynchronous measurements/actuation. We assume that  $y_s(t)$  is available for all  $t$ , while  $y_a(t)$  is sampled and only available at some time instants  $t_k$  where  $\{t_k \geq 0\}$  is a random increasing sequence of times. We assume that the measurement of the full state  $x(t_k)$  can be obtained from measurements  $y_s(t_k)$  and  $y_a(t_k)$ . Due to the asynchronous nature of  $y_a(t)$ , the time interval between two consecutive state measurements is unknown. A controller based on the asynchronous measurements  $y_a(t)$  must take into account that during consecutive state measurements, it has to operate in open-loop. This class of systems arises naturally in process control, where different process variables have to be measured such as temperature, flow or concentration. This model is also of interest for systems controlled through a hybrid communication network in which wireless sensors are used to add redundancy to existing working control loops (which use point-to-point wired communication links and continuous measurements) because wireless communication is often subject to data losses due to interference.

*Remark 1:* We have considered that the full state is available asynchronously for the controller  $u_a$  to simplify the notation. The results can be extended to controllers based on partial state information.

### C. Lower-tier Controller

The continuous measurement  $y_s(t)$  can be used to design a continuous output-feedback controller to stabilize the system. We term the control system based only on the continuous measurements  $y_s(t)$  as lower-tier controller. This control scheme does not use the asynchronous measurements  $y_a(t)$ . Figure 1 shows a schematic of the lower-tier controller. Following this idea, we assume that there exist an output feedback controller  $u_s(t) = k_s(y(t))$  that renders the origin of the nominal closed-loop system (i.e.,  $w(t) \equiv 0$ ) asymptotically stable with  $u_a(t) \equiv 0$ . Using converse Lyapunov theorems (see [19]), this assumption implies that there exist functions  $\alpha_i(\cdot)$ ,  $i = 1, 2, 3, 4$  of class  $\mathcal{K}^2$  and a Lyapunov function  $V$  for the nominal closed-loop system which is continuous and bounded in  $R^{n_x}$ , that satisfy the following inequalities

$$\begin{aligned}\alpha_1(|x|) &\leq V(x) \leq \alpha_2(|x|) \\ \frac{\partial V(x)}{\partial x} f(x, k_s(h_s(x)), 0, 0) &\leq -\alpha_3(|x|) \\ \left| \frac{\partial V(x)}{\partial x} \right| &\leq \alpha_4(|x|)\end{aligned}\quad (2)$$

for all  $x \in D \subseteq R^{n_x}$  where  $D$  is an open neighborhood of the origin. We denote the region  $\Omega_\rho \subseteq D$  as the stability

<sup>2</sup>Class  $\mathcal{K}$  functions are strictly increasing functions of their argument and satisfy  $\rho(0) = 0$ .

<sup>3</sup>We use  $\Omega_r$  to denote the set  $\Omega_r := \{x \in R^{n_x} | V(x) \leq r\}$ .

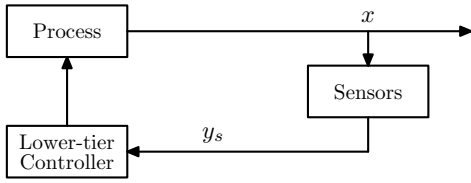


Fig. 1. Lower-tier controller with dedicated point-to-point, wired communication links and continuous sensing/actuation.

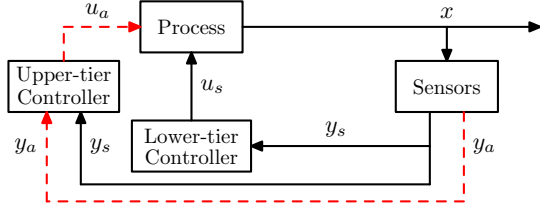


Fig. 2. Two-tier control strategy (solid lines denote dedicated point-to-point, wired communication links and continuous sensing/actuation; dashed lines denote networked (wired/wireless) communication and/or asynchronous sampling/actuation).

region of the closed-loop system under the controller  $k_s(y_s)$ . In the remainder, we will refer to the controller  $k_s$  as the lower-tier controller.

The lower-tier controller based on the output-feedback controller  $k_s$  is able to stabilize the system, however, it does not profit from the extra information  $y_a(t)$  and corresponding actuation  $u_a$ . In what follows, we propose a two-tier control architecture that profits from this extra information to improve the closed-loop performance.

*Remark 2:* We have considered static lower-tier controllers to simplify the notation. The formulation can be extended to dynamic lower-tier controllers. In the example in section IV, a proportional-integral (PI) controller is used as the lower-tier controller.

### III. TWO-TIER ARCHITECTURE AND LMPC DESIGN

#### A. Two-tier Architecture

The main objective of the two-tier control architecture is to improve the performance of the closed-loop system using the information provided by  $y_a(t)$  and corresponding actuation  $u_a$  while guaranteeing that the stability properties of the lower-tier controller are maintained. This is done by defining a controller (upper-tier controller) based on the full state measurements obtained from both the synchronous and asynchronous measurements at time steps  $t_k$ . The upper-tier controller decides the trajectory of  $u_a(t)$  between successive samples, i.e., for  $t \in [t_k, t_{k+1}]$ . Figure 2 shows a schematic of the proposed strategy. Due to the asynchronous nature of  $y_a(t)$ , the upper-tier controller has to take into account that the time interval between two consecutive samples is unknown and there exists the possibility of an infinitely large interval.

#### B. LMPC Design

In order to take advantage of the model of the system and the asynchronous state measurements, we propose to use model predictive control to decide  $u_a$ . The main idea

is the following: at each time instant  $t_k$  that a new state measurement is obtained, an open-loop finite horizon optimal control problem is solved and an optimal input trajectory is obtained. This input trajectory is implemented until a new measurement arrives at time  $t_{k+1}$ . If the time between two consecutive measurements is longer than the prediction horizon,  $u_a$  is set to zero until a new measurement arrives and the optimal control problem is solved again. In order to define a finite dimensional optimization problem,  $u_a$  is constrained to belong to the family of piece-wise constant functions with sampling period  $\Delta$ ,  $S(\Delta)$ . In order to guarantee that the resulting closed-loop system is stable, we follow a Lyapunov-based approach, see [20]. Lyapunov-based MPC (LMPC) is based on including a contractive constraint that allows one to prove practical stability. In previous LMPC controllers [21], [22], [20], the contractive constraints are defined based on a known Lyapunov-based state feedback controller. In the present work, the contractive constraint of the proposed upper-tier LMPC design is based on the lower-tier controller. The proposed upper-tier LMPC optimization problem is defined as follows:

$$\min_{u_a \in S(\Delta)} \int_0^{\tau_f} L(\tilde{x}(\tau), k_s(h_s(\tilde{x}(\tau))), u_a(\tau), 0) d\tau \quad (3a)$$

$$\dot{\tilde{x}}(\tau) = f(\tilde{x}(\tau), k_s(h_s(\tilde{x}(\tau))), u_a(\tau), 0) \quad (3b)$$

$$\dot{\hat{x}}(\tau) = f(\hat{x}(\tau), k_s(h_s(\hat{x}(\tau))), 0, 0) \quad (3c)$$

$$\hat{x}(0) = \tilde{x}(0) = x(t_k) \quad (3d)$$

$$V(\tilde{x}(t)) \leq V(\hat{x}(t)) \quad \forall t \in [0, \tau_f] \quad (3e)$$

where  $x(t_k)$  is the state obtained from both the measurements of  $y_s$  and  $y_a$ ,  $\tilde{x}$  is the predicted trajectory of the two-tier nominal system with the input trajectory computed by the LMPC,  $\hat{x}$  is the predicted trajectory of the two-tier nominal system with the input trajectory  $u_a(\tau) \equiv 0$  for all  $\tau \in [0, \tau_f]$ ,  $L(x, u_s, u_a)$  is a positive definite function of the state and the inputs that defines the cost, and  $\tau_f$  is the prediction horizon. This optimization problem does not depend on the uncertainty and assures that the system in closed-loop with the upper-tier controller maintains the stability properties of the lower-tier controller. The optimal solution to this optimization problem is denoted  $u_a^*(\tau|t_k)$ . This signal is defined for all  $\tau > 0$  with  $u_a^*(\tau|t_k) = 0$  for all  $\tau > \tau_f$ .

The control inputs of the proposed two-tier control architecture based on above LMPC are defined as follows:

$$\begin{aligned} u_s(t) &= k(h_s(x(t))), \quad \forall t \\ u_a(t) &= u_a^*(t - t_k|t_k), \quad \forall t \in [t_k, t_{k+1}] \end{aligned} \quad (4)$$

where  $u_a^*(t - t_k|t_k)$  is the optimal solution of the LMPC problem at time step  $t_k$ . This implementation technique takes into account that the lower-tier controller uses the continuously available measurements, while the upper-tier controller has to operate in open-loop between consecutive asynchronous measurements. Note that by definition,  $u_a^*(\tau|t_k) = 0$  for all  $\tau > \tau_f$ . This implies that the upper-tier controller switches off when it has been operating in open-loop for a time longer than its prediction horizon  $\tau_f$ .

*Remark 3:* Note that even the lower-tier controller can stabilize the closed-loop system, if the upper-tier controller is not carefully designed, integrating continuous and asynchronous measurements from a hybrid communication system may lead to loss of the stability properties achieved by the lower-tier controller because of the nonlinearity and asynchronous properties of the resulting closed-loop system [23].

*Remark 4:* Because of the introduction of the contractive constraint (3e) in the proposed upper-tier LMPC, it is guaranteed that the closed-loop system maintains the stability achieved by the lower-tier controller (please see Theorem 1 in section III-C). Moreover, if the Lyapunov function  $V$  has the same or similar structure as or with the performance index  $L$  (see the example in section IV in which  $V$  and  $L$  are both quadratic functions of  $x$ ), it is guaranteed that the closed-loop performance is better or no worse than the case when only the lower-tier controller is used. (This property follows once Theorem 1 is proved. To make the statement brief, it is not shown in this paper.)

### C. Two-tier Controller Stability

In this work, we follow a Lyapunov-based approach to prove the stability. The main idea is to compute the input  $u_a(t)$  applied to the system in a way such that the value of the Lyapunov function at time steps  $t_k$ ,  $V(x(t_k))$ , is a decreasing sequence of values with a lower bound. This guarantees practical stability of the closed-loop system. This is achieved thanks to the contractive constraint (3e) of the LMPC optimization problem. This property is presented in Theorem 1 below. To state this theorem, we need the following propositions:

*Proposition 1 (c.f. [19]):* Consider system (1) in closed-loop with the lower-tier controller. Taking into account (2), there exists a  $\mathcal{KL}^4$  function  $\beta(r, s)$  such that if  $x(0) \in \Omega_\rho$  and  $w(t) = 0$ ,  $u_a(t) = 0$  for all  $t$  then

$$V(x(t)) \leq \beta(V(x(0)), t).$$

This proposition provides us with a bound on the trajectories of the Lyapunov function of the state of the nominal system in closed-loop with the lower-tier controller with  $u_a(t) = 0$ .

*Proposition 2:* Consider the following state trajectories

$$\begin{aligned} \dot{x}_a(t) &= f(x_a(t), u_s(t), u_a(t), w(t)) \\ \dot{x}_b(t) &= f(x_b(t), u_s(t), u_a(t), 0) \end{aligned} \quad (5)$$

with initial states  $x_a(t_0) = x_b(t_0) \in \Omega_\rho$ . There exists a class  $\mathcal{K}$  function  $f_W(s)$  such that

$$|x_a(t) - x_b(t)| \leq f_W(t - t_0), \quad (6)$$

for all  $x_a(t), x_b(t) \in \Omega_\rho$  and all  $w(t) \in W$ .

*Proof:* Define the error vector as  $e(t) = x_a(t) - x_b(t)$ . The time derivative of the error is given by

$$\dot{e}(t) = f(x_a(t), u_s(t), u_a(t), 0) - f(x_b(t), u_s(t), u_a(t), 0).$$

<sup>4</sup>Function  $\beta(r, s)$  is said to be a class  $\mathcal{KL}$  function if, for each fixed  $s$ ,  $\beta(r, s)$  belongs to class  $\mathcal{K}$  function with respect to  $r$  and, for each fixed  $r$ ,  $\beta(r, s)$  is decreasing with respect to  $s$  and  $\beta(r, s) \rightarrow 0$  as  $s \rightarrow 0$ .

By continuity and the local Lipschitz property assumed for the vector field  $f(x, u_s, u_a, w)$ , there exist positive constants  $L_w$  and  $L_x$  such that

$$|\dot{e}(t)| \leq L_w|w(t) - 0| + L_x|x_a(t) - x_b(t)| \leq L_w\theta + L_x|e(t)|$$

for all  $x_a(t), x_b(t) \in \Omega_\rho$  and  $w(t) \in W$ . Integrating  $|\dot{e}(t)|$  with initial condition  $e(t_0) = 0$  (recall that  $x_a(t_0) = x_b(t_0)$ ), the following bound on the norm of the error vector is obtained

$$|e(t)| \leq \frac{L_w\theta}{L_x}(e^{L_x(t-t_0)} - 1).$$

This implies that (6) holds for

$$f_W(\tau) = \frac{L_w\theta}{L_x}(e^{L_x\tau} - 1). \quad \blacksquare$$

The following proposition bounds the difference between the magnitudes of the Lyapunov function of two different states in  $\Omega_\rho$ .

*Proposition 3:* Consider the Lyapunov function  $V(\cdot)$  of system (1). There exists a quadratic function  $f_V(\cdot)$  such that

$$V(x) \leq V(\hat{x}) + f_V(|x - \hat{x}|) \quad (7)$$

for all  $x, \hat{x} \in \Omega_\rho$ .

*Proof:* Because the Lyapunov function  $V(x)$  is continuous and bounded on compact sets, we can find a positive constant  $M$  such that a Taylor series expansion of  $V$  around  $\hat{x}$  yields

$$V(x) \leq V(\hat{x}) + \frac{\partial V}{\partial x}|x - \hat{x}| + M|x - \hat{x}|^2, \forall x, \hat{x} \in \Omega_\rho.$$

Note that the term  $M|x - \hat{x}|^2$  bounds the high order terms of the Taylor series of  $V(x)$  for all  $x, \hat{x} \in \Omega_\rho$ . Taking into account (2), the following bound for  $V(x)$  is obtained

$$V(x) \leq V(\hat{x}) + \alpha_4(\alpha_1^{-1}(\rho))|x - \hat{x}| + M|x - \hat{x}|^2, \forall x, \hat{x} \in \Omega_\rho.$$

This implies that (7) holds for  $f_V(x) = \alpha_4(\alpha_1^{-1}(\rho))x + Mx^2$ .  $\blacksquare$

*Theorem 1:* Consider system (1) in closed-loop with the two-tier control architecture (4). If  $x(t_0) \in \Omega_\rho$ , and there exist a concave function  $g$  such that

$$g(x) \geq \beta(x, \tau_f)$$

for all  $x \in \Omega_\rho$ , and a positive constant  $c \leq \rho$  such that

$$c - g(c) \geq f_V(f_W(\tau_f)), \quad (8)$$

then  $x(t)$  is ultimately bounded in a region that contains the origin.

*Proof:* In order to prove that the closed-loop system is ultimately bounded in a region that contains the origin, we will prove that  $V(x(t_k))$  is a decreasing sequence of values with a lower bound for the worst possible case, that is, the upper-tier controller always operates in open-loop for a period of time longer than  $\tau_f$  between consecutive samples, that is,  $t_{k+1} - t_k > \tau_f$  for all  $k$ . The trajectory  $\hat{x}(t)$  corresponds to the nominal system in closed-loop with

the lower-tier controller with initial state  $x(t_k)$ . Taking into account Proposition 1 the following inequality holds

$$V(\hat{x}(t)) \leq \beta(V(x(t_k)), t - t_k).$$

The contractive constraint of the proposed LMPC guarantees that

$$V(\tilde{x}(t)) \leq V(\hat{x}(t)), \forall t \in [t_k, t_k + \tau_f].$$

Assuming that  $x(t) \in \Omega_\rho$  for all times, we can apply Proposition 3 to obtain the following inequalities

$$V(x(t_k + \tau_f)) \leq V(\tilde{x}(t_k + \tau_f)) + f_V(|x(t_k) - \tilde{x}(t_k)|).$$

This assumption is automatically satisfied if the system is proved to be ultimately bounded. Applying Proposition 2 we obtain the following upper bounds on the deviation of  $\tilde{x}(t)$  from  $x(t)$

$$|x(t_k + \tau_f) - \tilde{x}(t_k + \tau_f)| \leq f_W(\tau_f).$$

Using these inequalities the following upper bound on  $V(x(t_k + \tau_f))$  is obtained:

$$V(x(t_k + \tau_f)) \leq \beta(V(x(t_k)), \tau_f) + f_V(f_W(\tau_f)). \quad (9)$$

Taking into account that the lower-tier controller renders the equilibrium point asymptotically stable (after  $t + \tau_f$ , the Lyapunov function is monotonically decreasing), and that for all  $t > t_k + \tau_f$  the upper-tier controller is switched off, i.e.,  $u_a(t) = 0$ , this implies that

$$V(x(t_{k+1})) \leq V(x(t_k + \tau_f))$$

for all  $w(t) \in W$ . Because function  $g$  is concave,  $z - g(z)$  is an increasing function. If there is a constant  $c \leq \rho$  satisfying (8), then (8) holds for all  $z > c$ . Taking into account that  $g(z) \leq \beta(z, \tau_f)$  for all  $z \leq \rho$ , the following inequality is obtained

$$z - \beta(z, \tau_f) \geq f_V(f_W(\tau_f))$$

when  $c \leq z \leq \rho$ . From this inequality and inequality (9), we obtain that

$$V(x(t_{k+1})) \leq V(x(t_k))$$

for all  $V(x(t_k)) \geq c$ . It follows using Lyapunov arguments that

$$\limsup_{t \rightarrow \infty} V(x(t)) \leq \rho_c$$

where

$$\rho_c = \max_c \beta(c, \tau_f) + f_V(f_W(\tau_f)).$$

*Remark 5:* Referring to Theorem 1, condition (8) puts a constraint on the combination of the values of  $\tau_f$ ,  $\theta$  and  $\Delta$ , under which the proposed two-tier control architecture (4) works. It implies that when  $\theta$  and  $\Delta$  are fixed, there is a maximum value for  $\tau_f$  which sets the maximum period of time in which the upper-tier controller can be operating in open-loop.

*Remark 6:* Although the proof of Theorem 1 is constructive, the constraints obtained are conservative. In practice, the parameters  $\tau_f$ ,  $\theta$  and  $\Delta$  are better estimated through

TABLE I  
PROCESS PARAMETERS

$F$	4.998 [ $m^3/h$ ]	$k_{10}$	$3 \cdot 10^6$ [ $h^{-1}$ ]
$V_r$	1 [ $m^3$ ]	$k_{20}$	$3 \cdot 10^5$ [ $h^{-1}$ ]
$R$	8.314 [ $KJ/kmol \cdot K$ ]	$k_{30}$	$3 \cdot 10^5$ [ $h^{-1}$ ]
$T_{A0}$	300 [ $K$ ]	$E_1$	$5 \cdot 10^4$ [ $KJ/kmol$ ]
$C_{A0s}$	4 [ $kmol/m^3$ ]	$E_2$	$7.53 \cdot 10^4$ [ $KJ/kmol$ ]
$\Delta H_1$	$-5.0 \cdot 10^4$ [ $KJ/kmol$ ]	$E_3$	$7.53 \cdot 10^4$ [ $KJ/kmol$ ]
$\Delta H_2$	$-5.2 \cdot 10^4$ [ $KJ/kmol$ ]	$\sigma$	1000 [ $kg/m^3$ ]
$\Delta H_3$	$-5.4 \cdot 10^4$ [ $KJ/kmol$ ]	$c_p$	0.231 [ $KJ/kg \cdot K$ ]

closed-loop simulations. The condition (8) is more useful as a guideline on the interaction among the various parameters that define the system.

#### IV. APPLICATION TO A CHEMICAL REACTOR

Consider a well mixed, non-isothermal continuous stirred tank reactor where three parallel irreversible elementary exothermic reactions take place of the form  $A \rightarrow B$ ,  $A \rightarrow C$  and  $A \rightarrow D$ .  $B$  is the desired product and  $C$  and  $D$  are byproducts. The feed to the reactor consists of  $A$  at temperature  $T_{A0}$  and  $C_{A0}$  and flow rate  $F + \Delta F$ , where  $\Delta F$  is a time-varying uncertainty. Due to the non-isothermal nature of the reactor, a jacket is used to remove/provide heat from/to the reactor. Using first principles and standard modeling assumptions the following mathematical model of the process is obtained

$$\begin{aligned} \frac{dT}{dt} &= \frac{F + \Delta F}{V_r} (T_{A0} - T) - \sum_{i=1}^3 \frac{\Delta H_i}{\sigma c_p} k_{i0} e^{-\frac{E_i}{RT}} C_A + \frac{Q}{\sigma c_p V_r} \\ \frac{dC_A}{dt} &= \frac{F + \Delta F}{V_r} (C_{A0} - C_A) + \sum_{i=1}^3 k_{i0} e^{-\frac{E_i}{RT}} C_A + \frac{F}{V_r} \Delta C_{A0} \end{aligned} \quad (10)$$

where  $C_A$  denotes the concentration of the reactant  $A$ ,  $T$  denotes the temperature of the reactor,  $V_r$  denotes the volume of the reactor,  $\Delta H_i$ ,  $k_{i0}$ ,  $E_i$ ,  $i = 1, 2, 3$  denote the enthalpies, pre-exponential constants and activation energies of the three reactions, respectively, and  $c_p$  and  $\sigma$  denote the heat capacity and the density of the fluid in the reactor. The inputs to the system are the rate of heat input/removal  $Q$  and the change of the inlet reactant  $A$  concentration  $\Delta C_{A0}$ . The values of the process parameters are shown in Table I.

System (10) has three steady-states (two locally asymptotically stable and one unstable). The control objective is to stabilize the system at the open-loop unstable steady-state  $T_s = 388$  K,  $C_{As} = 3.59$  mol/l. The flow rate uncertainty is bounded by  $|\Delta F| \leq 3$  m<sup>3</sup>/h.

We assume that the measurement of temperature  $T$  is available continuously, and the measurements of the concentration  $C_A$  are available asynchronously at time instants  $\{t_{k \geq 0}\}$ . We also assume that there exists a lower bound  $T_{min}$  on the time interval between two consecutive concentration measurements.

In order to model the time sequence  $\{t_{k \geq 0}\}$  we use a random Poisson process. The Poisson process is defined by the number of events per unit time  $W$ . The interval between two consecutive concentration sampling times (events of the Poisson process) is given by  $\Delta_a = \frac{-\ln \chi}{W}$ , where  $\chi$

is a random variable with uniform probability distribution between 0 and 1. The sequence  $\{t_{k \geq 0}\}$  for a simulation of length  $t_f$  is generated as follows:

```

 $t_0 = 0, k = 0$ 
while  $t_k < t_f$ 
   $\chi = rand(1)$ 
   $t_{k+1} = t_k + \frac{-\ln \chi}{W}$ 
  if  $t_{k+1} < t_k + T_{min}$ , then  $t_{k+1} = t_k + T_{min}$ 
   $k = k + 1$ 
end

```

where  $rand(1)$  generates a uniformly distributed random value  $\chi$  between 0 and 1,  $T_{min}$  is the minimum time interval between two consecutive samplings. For the simulations carried out in this section we pick the value of the minimum time interval to be  $T_{min} = 0.025 \text{ hr} = 1.5 \text{ min}$ , which is meaningful from a practical point of view with respect to concentration measurements.

The process model (10) belongs to the class of nonlinear systems described by system (1) where  $x^T = [x_1 \ x_2] = [T - T_s \ C_A - C_{As}]$  is the state,  $u_s = Q$  and  $u_a = \Delta C_{A0}$  are the manipulated inputs,  $\theta = \Delta F$  is a time varying bounded disturbance,  $y_s = x_1 = T - T_s$  is the continuous temperature measurement and  $y_a = x_2 = C_A - C_{As}$  is the asynchronously sampled concentration measurement.

An output feedback controller (lower-tier controller) based on the continuous temperature measurements (i.e.,  $x_1(t)$ ) is first designed to stabilize system (10) using only the rate of heat input  $u_s = Q$  as the manipulated input. The manipulated input is bounded by  $|u_s| \leq 10^5 \text{ KJ/h}$ . In particular, the following proportional-integral (PI) control law is used as the lower-tier controller:

$$u_s(t) = k_s(x_1(t)) \quad (11)$$

with  $k_s(x_1(t)) = K(x_1 + \frac{1}{T_i} \int_0^t x_1 dt)$  where  $K$  is the proportional gain and  $T_i$  is the integral time constant. To compute the parameters of the PI controller, the linearized model  $\dot{x} = Ax + Bu_s$  of system (10) around the equilibrium point is obtained. The proportional gain  $K$  is chosen to be  $-8100$ . This value guarantees that the origin of  $\dot{x} = (A + BK[1 \ 0])x$  is asymptotically stable with its eigenvalues being  $\lambda_1 = -1.06 \times 10^5$  and  $\lambda_2 = -4.43$ . A quadratic Lyapunov function  $V(x) = x^T P x$  with

$$P = \begin{bmatrix} 0.024 & 5.21 \\ 5.21 & 1.13 \times 10^3 \end{bmatrix}$$

is obtained by solving an algebraic Lyapunov equation  $A_c^T P + P A_c + Q_c = 0$  for  $P$  with  $A_c = A + BK[1 \ 0]$ . This Lyapunov function will be used to design the upper-tier LMPC controller. The integral time constant is chosen to be  $T_i = 49.6 \text{ hr}$ . For simplicity, the Lyapunov function  $V(x)$  is determined on the basis of the closed-loop system under the proportional (P) term of the PI controller only; the effect of the integral (I) term is very small for the specific choice of the controller parameters used in the simulations. The state and input trajectories of system (10) starting from  $x_0 = [370 \ 3.41]^T$  under the PI controller are shown in Fig. 3. From Fig. 3, we see that the PI controller (11) stabilizes

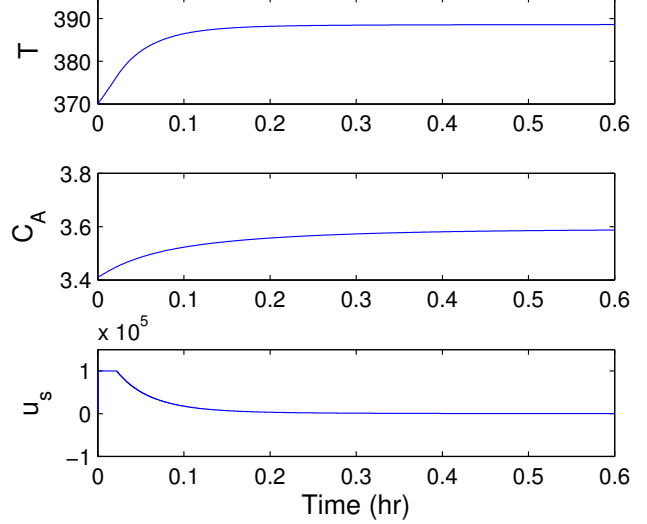


Fig. 3. State and input trajectories of system (10) under lower-tier PI control (11).

the temperature and concentration of system (10) at the equilibrium point in about 0.2 hr and 0.3 hr, respectively.

We have implemented the proposed two-tier control architecture to improve the performance of the closed-loop system. In this set of simulations, the PI controller (11) is used as the lower-tier controller. Instead of abandoning the less frequent concentration measurement, we take advantage of both the continuous measurements of the temperature  $T$  and the asynchronous concentration measurements  $C_A$  together with the nominal model of system (10) to design the upper-tier LMPC. The inlet concentration change  $\Delta C_{A0}$  is the manipulated input for the LMPC.

The LMPC is designed next. The performance index is defined by the following positive definite function

$$L(x, u_s, u_a) = x^T Q_c x \quad (12)$$

where  $x$  is the state of the system and  $Q_c$  is the following weight matrix

$$Q_c = \begin{bmatrix} 1 & 0 \\ 0 & 10^4 \end{bmatrix}.$$

The values of the weights in  $Q_c$  have been chosen to account for the different range of numerical values for each state. The sampling time of the LMPC is  $\Delta = 0.025 \text{ hr}$  which is the same as  $T_{min}$ ; the prediction horizon is chosen to be  $\tau_f = 11\Delta$  so that the prediction captures most of the dynamic evolution of the process; the quadratic control Lyapunov function  $V(x)$  is used in the design of the contractive constraint (3e) and the inlet concentration change  $\Delta C_{A0}$  is bounded by  $|u_a = \Delta C_{A0}| \leq 1 \text{ kmol/m}^3$ .

The two-tier control architecture is implemented as discussed in the previous section. The lower-tier controller uses the continuous temperature measurements to control  $u_s(t)$ . When the measurements of  $T$  and  $C_A$  are obtained at time instant  $t_k$ , an estimate of the state of system (10),  $x_e(t_k)$ , is

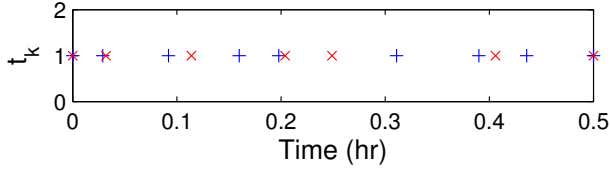


Fig. 4. Concentration sampling times, +: sampling times generated with  $W = 30$ ,  $\times$ : sampling times generated with  $W = 20$ .

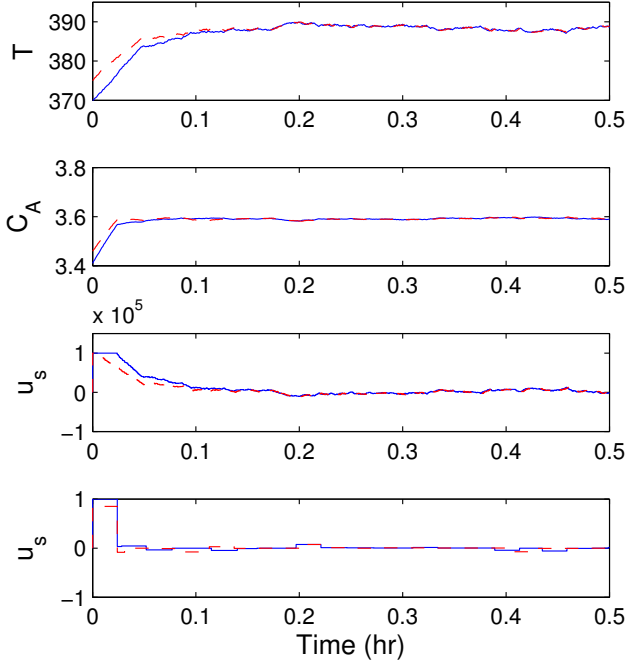


Fig. 5. State and inputs trajectories of system (10) under the proposed two-tier control architecture when  $W = 30$  (solid curves) and  $W = 20$  (dashed curves).

obtained by integrating the two measurements using the process model. Based on the estimated state  $x_e(t_k)$ , the LMPC optimization problem (3) is solved and an optimal input trajectory  $u_a^*(\tau|t_k)$  is obtained. This optimal input trajectory is implemented until a new concentration measurement is obtained at time  $t_{k+1}$  (note that  $k$  indexes the number of concentration samples received, not a given sampling time). Note that because a PI controller is used in the lower-tier, we need to predict the controller dynamics (the control effects generated by the integral part) in the optimization problem of the proposed LMPC scheme (3).

The stability and robustness of the two-tier control architecture (4) have been studied with two different initial conditions  $x(0) = [370 \ 3.41]^T$  and  $x(0) = [375 \ 3.46]^T$  associated with two different concentration measurements sequences  $\{t_{k>0}\}$  (see Fig. 4) generated with  $W = 30$  and  $W = 20$ , respectively. The average time intervals between two consecutive sampling times are  $0.0625 \text{ hr}$  for  $W = 30$  and  $0.0833 \text{ hr}$  for  $W = 20$ . In addition, two different disturbance trajectories of  $w(t)$  with a random value at each simulation step are added to the closed-loop system. The state and inputs trajectories of system (10) under the proposed two-tier control architecture are shown in Fig. 5.

TABLE II

TOTAL PERFORMANCE COST ALONG THE CLOSED-LOOP TRAJECTORIES.

sim.	Two-Tier	PI Controller	sim.	Two-Tier	PI Controller
1	203.92	704.54	11	224.03	831.63
2	188.74	815.47	12	203.78	738.47
3	198.33	922.87	13	265.44	617.15
4	221.76	640.87	14	210.58	704.95
5	240.44	656.47	15	190.68	723.05
6	226.44	847.43	16	209.66	695.60
7	199.19	779.03	17	205.90	808.71
8	233.40	736.65	18	211.29	749.24
9	200.45	702.26	19	214.79	737.62
10	198.74	753.25	20	217.13	813.70

From Fig. 5, we see that the two-tier control architecture (4) stabilizes the temperature and concentration of the system in about  $0.1 \text{ hr}$  and  $0.05 \text{ hr}$  respectively. This implies that the resulting closed-loop system response is faster. Moreover, the cost associated with the resulting closed-loop trajectories is lower.

Another set of simulations was carried out to compare the proposed two-tier control architecture with the lower-tier PI control system from a performance index point of view. Table II shows the total cost computed for 20 different closed-loop simulations under the proposed two-tier control architecture and the PI control scheme. To carry out this comparison, we have computed the total cost of each simulation based on the integral of the performance index defined by  $L(x, u_s, u_a)$  from the initial time to the end of the simulation  $t_f = 0.5 \text{ hr}$ . For this set of simulations  $W$  is chosen to be 10. For each pair of simulations (one for each controller) a different initial state inside the stability region, a different uncertainty trajectory and a different random concentration measurement sequence is chosen. As it can be seen in Table II, the proposed two-tier control architecture has a cost lower than the corresponding total cost under the PI controller in all the simulations.

We have also carried out another set of simulation to compare the proposed two-tier scheme with a controller based on using the measurements of  $T$  and  $C_A$  to decide both control inputs  $u_s$  and  $u_a$  in an LMPC framework. This controller is based on solving an LMPC optimization problem that optimizes both  $u_s(\tau|t_k)$  and  $u_a(\tau|t_k)$  when a new full state measurement is available at time step  $t_k$ . It based on the following optimization problem

$$\begin{aligned}
 \min_{u_a, u_s \in S(\Delta)} \quad & \int_0^{\tau_f} L(\tilde{x}(\tau), u_s(\tau), u_a(\tau)) d\tau \\
 \dot{\tilde{x}}(\tau) = \quad & f(\tilde{x}(\tau), u_s(\tau), u_a(\tau), 0) \\
 \hat{\tilde{x}}(\tau) = \quad & f(\hat{x}(\tau), k_s(h_s(\hat{x}(j\Delta))), 0, 0) \\
 \forall \tau \in \quad & [j\Delta, (j+1)\Delta], \\
 \hat{\tilde{x}}(0) = \quad & \tilde{x}(0) = x_e(t_k) \\
 V(\tilde{x}(t)) \leq \quad & V(\hat{x}(t)) \quad \forall t \in [0, \tau_f].
 \end{aligned}$$

which was proposed in [20] for system subject to measurement data losses and asynchronous measurements. We denote this controller as single-tier LMPC. It applies both  $u_s$  and  $u_a$  in a sample and hold fashion and its optimal input trajectories are applied in open-loop until a new full state measurement is available, which implies that it does not profit from the continuous temperature measurements. The

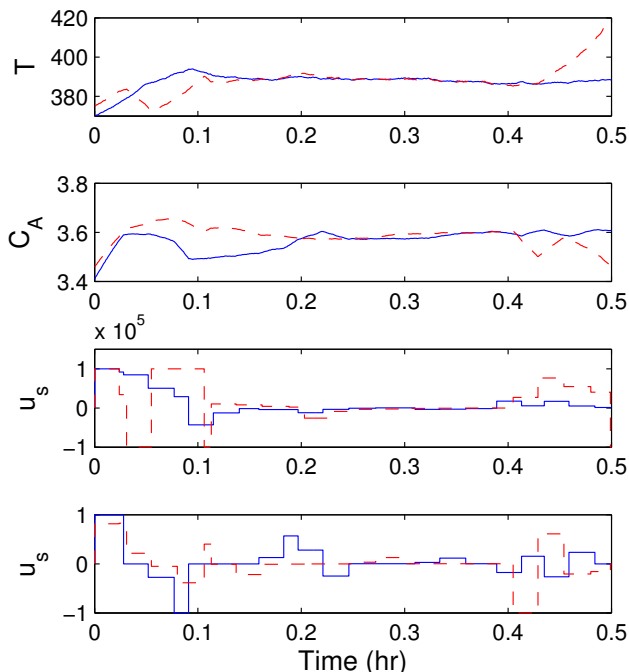


Fig. 6. State and inputs trajectories of system (10) under the single-tier LMPC scheme with concentration sampling times generated with  $W = 30$  (solid curves) and  $W = 20$  (dashed curves).

single-tier LMPC is also based on the PI controller (11) to design the contractive constraint (although in a sample and hold fashion), however, the applied  $u_a(t)$  is not decided using the lower-tier controller, but the solution of the optimization problem, that is

$$\begin{aligned} u_s(t) &= u_s^*(t - t_k | t_k), \quad \forall t \in [t_k, t_{k+1}) \\ u_a(t) &= u_a^*(t - t_k | t_k), \quad \forall t \in [t_k, t_{k+1}). \end{aligned}$$

For these simulations, the single-tier LMPC uses the same controller parameters, initial conditions, concentration sampling times (see Fig. 4) and disturbance trajectories as the ones used in the two-tier control architecture. The state and inputs trajectories of the closed-loop system under the single-tier LMPC scheme are shown in Fig. 6. From the figure, it can be seen that the single-tier LMPC stabilizes the system (solid curves) when the time intervals between two consecutive measurements are small ( $0.0625 \text{ hr}$ ), but loses stability and can not stabilize the system (dashed curves) when these time intervals get bigger ( $0.0833 \text{ hr}$ ). The results are expected because the single-tier LMPC scheme does not profit from the continuous measurements of the temperature, thus, the stability region of the closed-loop system is in general reduced to a much smaller one compared to that obtained under the two-tier control architecture.

*Remark 7:* We considered a performance index  $L(x, u_s, u_a)$  that only penalizes the closed-loop system state and not the control action because the two-tier control architecture utilizes different manipulated inputs from the lower-tier controller. Since the performance index has only penalty on the closed-loop system state, we have included an input constraint on the upper-tier manipulated input to

avoid computation of unnecessarily large control actions by the upper-tier controller (i.e.,  $|u_a| \leq 1 \text{ kmol/m}^3$ ).

## REFERENCES

- [1] E. B. Ydstie, "New vistas for process control: Integrating physics and communication networks," *AIChE Journal*, vol. 48, pp. 422–426, 2002.
- [2] J. F. Davis, "Report from NSF Workshop on Cyberinfrastructure in Chemical and Biological Systems: Impact and Directions, (see <http://www.oit.ucla.edu/nsfci/NSFCIFullReport.pdf> for the pdf file of this report)," 2007.
- [3] P. D. Christofides, J. F. Davis, N. H. El-Farra, D. Clark, K. R. D. Harris, and J. N. Gipson, "Smart plant operations: Vision, progress and challenges," *AIChE Journal*, Perspective article, vol. 53, pp. 2734–2741, 2007.
- [4] R. W. Brockett and D. Liberzon, "Quantized stabilization of linear systems," *IEEE Transactions on Automatic Control*, vol. 45, pp. 1279–1289, 2000.
- [5] G. N. Nair and R. J. Evans, "Stabilization with data-rate-limited feedback: Tightest attainable bounds," *Systems & Control Letters*, vol. 41, 2000.
- [6] K. G. Shin, "Real-time communications in a computer-controlled workcell," *IEEE Transactions on Robotics and Automation*, vol. 7, pp. 105–113, 1991.
- [7] S. H. Hong, "Scheduling algorithm of data sampling times in the integrated communication and control-systems," *IEEE Transactions On Control Systems Technology*, vol. 3, pp. 225–230, 1995.
- [8] G. Walsh, H. Ye, and L. Bushnell, "Stability analysis of networked control systems," *IEEE Transactions On Control Systems Technology*, vol. 10, pp. 438–446, 2002.
- [9] D. Nesić and A. R. Teel, "Input-to-state stability of networked control systems," *Automatica*, vol. 40, 2004.
- [10] M. Tabbara, D. Nesić, and A. R. Teel, "Stability of wireless and wireline networked control systems," *IEEE Transactions on Automatic Control*, vol. 52, pp. 1615–1630, 2007.
- [11] V. S. Ritzchev and G. F. Franklin, "A stability criterion for asynchronous multirate linear systems," *IEEE Transactions on Automatic Control*, vol. 34, pp. 529–535, 1989.
- [12] Y. F. Su, A. Bhaya, E. Kaszkurewicz, and V. S. Kozyakin, "Further results on stability of asynchronous discrete-time linear systems," in *Proc. IEEE Conf. Decision and Control*, San Diego, CA, 1997, pp. 915–920.
- [13] G. T. Nguyen, R. H. Katz, B. Noble, and M. Satyanarayanan, "A tracebased approach for modeling wireless channel behavior," in *Proc. Winter Simulation Conference*, 1996, pp. 597–604.
- [14] J. P. Hespanha, "A model for stochastic hybrid systems with application to communication networks," *Nonlinear Analysis-Theory Methods and Applications*, vol. 62, pp. 1353–1383, 2005.
- [15] X. Mao, "Stability of stochastic differential equations with markovian switching," *Stochastic Processes and their Applications*, vol. 79, pp. 45–67, 1999.
- [16] A. Hassibi, S. P. Boyd, and J. P. How, "Control of asynchronous dynamical systems with rate constraints on events," in *Proc. IEEE Conf. Decision and Control*, 1999, pp. 1345–1351.
- [17] R. Findeisen and P. Varutti, "Stabilizing nonlinear predictive control over nondeterministic communication networks," in *Proc. Int. Workshop Assessment and Future Directions of Nonlinear Model Predictive Control*, 2008.
- [18] G. Pin and T. Parisini, "Stabilization of networked control systems by nonlinear model predictive control: a set invariance approach," in *Proc. Int. Workshop Assessment and Future Directions of Nonlinear Model Predictive Control*, 2008.
- [19] H. K. Khalil, *Nonlinear Systems, 2nd edition*. Prentice Hall, 1996.
- [20] D. Muñoz de la Peña and P. D. Christofides, "Lyapunov-based model predictive control of nonlinear systems subject to data losses," *IEEE Transactions on Automatic Control*, vol. 53, pp. 2076–2089, 2008.
- [21] P. Mhaskar, N. H. El-Farra, and P. D. Christofides, "Predictive control of switched nonlinear systems with scheduled mode transitions," *IEEE Transactions on Automatic Control*, vol. 50, pp. 1670–1680, 2005.
- [22] —, "Stabilization of nonlinear systems with state and control constraints using Lyapunov-based predictive control," *Systems & Control Letters*, vol. 55, pp. 650–659, 2006.
- [23] D. Muñoz de la Peña and P. D. Christofides, "Stability of nonlinear asynchronous systems," *Syst. & Contr. Lett.*, vol. 57, pp. 465–473, 2008.